The Case of a Cu_4 Rhombus in Molecular Magnetism: Preparation, Crystal Structure, and Magnetic Properties of $[Cu_4(dpk{\cdot}CH_3O)_4(CH_3O)_2](ClO_4)_2$ (dpk·CH_3OH = Monomethylated Diol of Di-2-pyridyl Ketone), an Example of a Cluster Allowing the Determination of All Its Exchange Parameters, Ranging from Very Strong to Very Weak

Vasilis Tangoulis,[†] Catherine P. Raptopoulou,[†] Sofia Paschalidou,[‡] Alexandros E. Tsohos,[†] Evangelos G. Bakalbassis,*[,§] Aris Terzis,*[,†] and Spyros P. Perlepes*[,‡]

Institute of Materials Science, NCSR "Demokritos", 153 10 Aghia Paraskevi Attikis, Greece, Department of Chemistry, University of Patras, 265 00 Patras, Greece, and Laboratory of Applied Quantum Chemistry, Department of General and Inorganic Chemistry, Faculty of Chemistry, Aristotle University of Thessaloniki, 540 06 Thessaloniki, Greece

Received March 20, 1997[⊗]

Treatment of $[Cu_2(O_2CCH_3)_4(H_2O)_2]$ with 2 equiv of di-2-pyridyl ketone (dpk) in methanol followed by addition of 1 equiv of $NaClO_4$ yields $[Cu_4(dpk{\cdot}CH_3O)_4(CH_3O)_2](ClO_4)_2$ (**1**) in ∼75% yield (dpk·CH_3O^- = the monoanion of the monomethylated diol of dpk). The same complex has also been isolated from the 1:2:2 and 1:4:4 stoichiometries. The 1:2 reaction of $Cu(ClO_4){\cdot}6H_2O$ with dpk in methanol affords the mononuclear complex $[Cu(dpk{\cdot}CH_3OH)_2](ClO_4)_2{\cdot}2CH_3OH$ (**2**) in ∼70% yield. Complex **1**, $C_{50}H_{50}Cl_2Cu_4N_8O_{18}$, crystallizes in the tetragonal space group $I4_1/acd$ with $a = b = 15.551(1)$ Å, $c = 48.938(3)$ Å, and $Z = 8$. Crystal data for **2**: $C_{26}H_{32}Cl_2CuN_4O_{14}$, monoclinic, space group $P2_1/a$, $a = 12.923(1)$ Å, $b = 12.969(2)$ Å, $c = 9.655(1)$ Å, $\beta = 92.78(1)°$, $Z = 2$. The four Cu^{II} atoms in the cation of **1** are all coplanar, exhibiting a rhombic arrangement. The dpk·CH_3O^- ion behaves as a $\eta^1{:}\eta^2{:}\eta^1{:}\mu_2$ ligand. In the cation of **2**, the dpk·CH_3OH ligand functions as a tridentate chelate toward the copper center, with the pyridyl nitrogens and the methylated oxygen being the ligated atoms. The magnetic properties of compound **1** are characteristic of prevailing antiferromagnetic interactions. The susceptibility data of **1** were fitted with a 3-*J* magnetic model, affording a very strong antiferromagnetic interaction ($J_2 = -490(9)$ cm^{-1}), a weak ferromagnetic interaction ($J_1 = +22(4)$ cm^{-1}), and a very weak antiferromagnetic interaction ($J_3 = -0.36(1)$ cm^{-1}). The energy spectrum of the states, the magnetization, and the EPR data of complex **1** are in line with an almost degenerate ground state with a magnetic component. An investigation of this degeneration is attempted.

Introduction

The study of tetranuclear copper(II) complexes with planar cyclic structures seems to be of great importance mainly due to the search for molecular precursor complexes to synthesize high-temperature superconductors.[1] The 1−2−3 superconductor has a layered structure.[1,2] In the unit cell these layers are $Cu_4O_2-BaO_4-Cu_4O_4-Y-Cu_4O_4-BaO_4-Cu_4O_2$; *i.e.*, the complex consists of Cu_4O_x units interlayered by BaO_4 and Y units. If molecular complexes with planar Cu_4O_x structures can be synthesized, they could be used as building blocks for the synthesis of molecular complexes with structure resembling that of the 1−2−3 superconductor in one dimension. Such building blocks will also make it possible to control the addition of different metal atoms to these complexes.[1] However, very few compounds with planar cyclic Cu_4 cores have been fully characterized, their magnetostructural correlation being still unknown.[1,3]

Herein we report the preparation and magnetochemical characterization of the interesting planar tetranuclear cluster $[Cu_4(dpk{\cdot}CH_3O)_4(CH_3O)_2](ClO_4)_2$ (**1**), where dpk·CH_3O^- is the monoanion of the monomethylated diol (**I**) of di-2-pyridyl ketone (dpk, **II**). Complex **1** is the first example of a planar

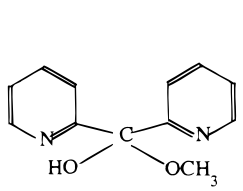

I, dpk.CH_3OH

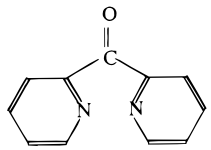

II, dpk

tetranuclear copper(II) complex in which the four magnetic ions occupy the apices of an "ideal" rhombus, in which the short diagonal is equal to the sides of the rhombus. This unusual rhombic arrangement could be considered as originating from two equilateral triangles[4] sharing a common edge. To the best of our knowledge, the peculiar planar arrangement of metal ions in **1** constitutes one of few examples in the molecular magnetism of Cu(II) in which both very strong and very weak exchange interactions can be easily determined. Also described in this paper are the preparation and characterization of the monomeric complex $[Cu(dpk{\cdot}CH_3OH)_2](ClO_4)_2$, the second example of a complex containing the neutral molecule dpk·CH_3OH as ligand.

[†] NCSR "Demokritos".
[‡] University of Patras.
[§] Aristotle University of Thessaloniki.
[⊗] Abstract published in *Advance ACS Abstracts,* October 1, 1997.

(1) Wang, S.; Trepanier, S. J.; Zheng, J. C.; Pang, Z.; Wagner, M. J. *Inorg. Chem.* **1992**, *31*, 2118.
(2) (a) Poole, C. P., Jr.; Datta, T.; Farach, H. A. *Copper Oxide Superconductors*; John Wiley and Sons: New York, 1988. (b) Rao, C. N. R; Ganguli, A. K. *Chem. Soc. Rev.* **1995**, 1. (c) Armstrong, A. R; David, W. I. F. *Chem. Br.* **1994**, 727.
(3) Murray, K. S. *Adv. Inorg. Chem.* **1995**, *43*, 261 and references therein.
(4) Beckett, R.; Colton, R.; Hoskins, F. F.; Martin, R. L.; Vince, G. G. *Aust. J. Chem.* **1969**, *22*, 2527.

S0020-1669(97)00332-7 CCC: $14.00

Experimental Section

Compound Preparations. The chemical synthesis was performed under aerobic conditions using Aldrich starting materials as received. Solvents were dried and distilled before use.

Caution! Perchlorate salts are potentially explosive. Only small quantities of these compounds should be prepared and handled behind suitable protective shields.

$[Cu_4(dpk{\cdot}CH_3O)_4(CH_3O)_2](ClO_4)_2$ (1). Solid $[Cu_2(O_2CCH_3)_4(H_2O)_2]$ (0.24 g, 0.6 mmol) was dissolved with stirring in a solution of dpk (0.22 g, 1.2 mmol) in warm MeOH (35 mL). A deep blue homogeneous solution was obtained, and to this was added a solution of $NaClO_4$ (0.08 g, 0.6 mmol) in MeOH (10 mL). No noticeable color change occurred. The solution was allowed to stand undisturbed at room temperature overnight. The resultant blue microcrystalline solid was collected by filtration, washed with a small amount of cold MeOH and Et_2O (2 × 5 mL), and dried *in vacuo* over P_4O_{10}. Typical yields are in the 70−80% range. Anal. Calcd for $C_{50}H_{50}Cl_2Cu_4N_8O_{18}$: C, 43.64; H, 3.67; N, 8.14; Cu, 18.47. Found: C, 43.52; H, 3.72; N, 8.26; Cu, 18.80. Selected IR data (KBr pellet, cm^{-1}): 2918 (w), 2814 (w), 1604 (m), 1470 (m), 1212 (m), 1114 (vs), 1096 (vs), 1052 (vs), 798 (s), 688 (m), 624 (m), 430 (m), 396 (w, br), 338 (s, br), 277 (m, br), 261 (m), 230 (m). Electronic spectrum in DMF (green solution), λ_{max}, nm (ϵ_M, L mol^{-1} cm^{-1}): 355 (∼25 000), 700 (386). Crystals of **1** suitable for X-ray structure analysis were obtained in MeOH using an H-shaped tube. Complex **1** can also be isolated by employing a $[Cu_2(O_2CCH_3)_4(H_2O)_2]$:dpk:$ClO_4^-$ molar ratio of 1:2:2 or 1:4:4 in MeOH.

$[Cu(dpk{\cdot}CH_3OH)_2](ClO_4)_2{\cdot}2CH_3OH$ (2). To a stirred solution of dpk (0.20 g, 1.08 mmol) in MeOH (25 mL) was added a blue solution of $Cu(ClO_4)_2{\cdot}6H_2O$ (0.20 g, 0.54 mmol) in the same solvent (25 mL). The resulting violet solution was allowed to slowly concentrate by evaporation at room temperature for 48 h. A violet microcrystalline solid was deposited, which was collected by filtration, washed with a small amount of cold MeOH, and dried *in vacuo* over P_4O_{10}. Yield: 0.28 g (68%). Drying under vacuum gives the methanol-free form. Anal. Calcd for $C_{24}H_{24}Cl_2CuN_4O_{12}$: C, 41.47; H, 3.49; N, 8.06; Cu, 9.14. Found: C, 41.62; H, 3.70; N, 8.01; Cu, 9.80. Selected IR data (KBr pellet, cm^{-1}): 3456 (m, br), 1608 (m), 1573 (w), 1470 (m), 1446 (m), 1308 (m), 1092 (vs, br), 1046 (s), 1030 (s), 764 (m), 738 (w), 652 (w), 626 (m). Electronic spectrum in MeOH, λ_{max}, nm (ϵ_M, L mol^{-1} cm^{-1}): 335 (∼2000), 596 (80). Solid-state effective magnetic moment: μ_{eff} = 1.92 μ_B (∼25 °C). To obtain crystals suitable for diffractometry, the initial, methanolic reaction solution was layered with a 1:1 mixture of hexane and Et_2O.

Physical Measurements. Elemental analyses (C, H, N) were performed at the Microanalytical Laboratory, Department of Chemistry, University of Dortmund, Germany. Copper analysis was carried out by EDTA titration. Infrared spectra (4000−500 cm^{-1}) were recorded as KBr pellets using a Perkin-Elmer 16 PC FT spectrophotometer. Far-infrared spectra (500−50 cm^{-1}) of **1** were recorded on a Bruker IFS 113v FT spectrophotometer with samples prepared as polyethylene pellets. Solution electronic spectra (800−300 nm) were recorded on a Biochrom 4060 instrument. EPR spectra were recorded in the 295−5 K temperature range on a Bruker ER 200D-SRC X-band spectrometer equipped with an Oxford ESR 9 cryostat. Variable-temperature magnetic susceptibility measurements were carried out on a polycrystalline sample of **1** in the 300−3.0 K temperature range using a Quantum Design SQUID susceptometer by applying magnetic fields of 1000 and 6000 G. Magnetization measurements were carried out at 3 K in the 0−5 T magnetic field range. The correction for the diamagnetism of the complex was estimated from Pascal's constants; a value of 60 × 10^{-6} cm^3 mol^{-1} was used for the TIP of the Cu(II) ion. The magnetism of the sample was found to be field independent.

X-ray Crystallography. A blue prismatic crystal of **1** with approximate dimensions 0.15 × 0.30 × 0.50 mm and a reddish purple prismatic crystal of **2** with approximate dimensions 0.15 × 0.30 × 0.55 mm were mounted in air and in a capillary filled with drops of mother liquid, respectively. Diffraction measurements for **1** were made on a Crystal Logic dual goniometer diffractometer using graphite-monochromated Mo radiation and for **2** on a $P2_1$ Nicolet diffractometer upgraded by Crystal Logic using Zr-filtered Mo radiation. Complete crystal data and parameters for data collection are reported in Table 1. Unit cells dimensions were determined and refined by using the angular settings of 25 automatically centered reflections in the range 11° < 2θ < 23°. Intensity data were recorded using a $\theta-2\theta$ scan to 2θ(max) = 50° with scan speeds of 2.0°/min for **1** and 3.0°/min for **2** and scan ranges of 2.4 and 2.5 (for **1** and **2**, respectively) plus $\alpha_1-\alpha_2$ separations. Three standard reflections, monitored every 97 reflections showed less than 3% intensity fluctuation and no decay. Lorentz, polarization, and ψ-scan absorption corrections were applied using Crystal Logic software.

Table 1. Crystallographic Data for Complexes **1** and **2**

	1	**2**
formula	$C_{50}H_{50}Cl_2Cu_4N_8O_{18}$	$C_{26}H_{32}Cl_2CuN_4O_{14}$
a, Å	15.551(1)	12.923(1)
b, Å	15.551(1)	12.969(2)
c, Å	48.938(3)	9.655(1)
β, deg		92.78(1)
V, Å^3	11834.8(1)	1616.4(3)
Z	8	2
fw	1376.04	759.00
space group	$I4_1/acd$	$P2_1/a$
T, °C	25	25
λ, Å	0.710 70	0.710 70
ρ_{obsd}, g cm^{-3}	1.53(2)	1.54(2)
ρ_{calcd}, g cm^{-3}	1.545	1.559
μ(Mo Kα), mm^{-1}	1.583	0.914
*R*1	0.0581	0.0534
w*R*2[a]	0.1450	0.1405

[a] $w = 1/[\sigma^2(F_o^2) + (aP)^2 + bP]$ and $P = (\max(F_o^2, 0) + 2F_c^2)/3$. a = 0.0678, b = 46.4749 for **1**, and a = 0.0823, b = 2.2695 for **2**. $R1 = \sum(|F_o| - |F_c|)/\sum(|F_o|)$ and $wR2 = \{\sum[w(F_o^2 - F_c^2)^2]/\sum[w(F_o^2)^2]\}^{1/2}$ for 1819 (**1**) and 1905 (**2**) reflections with $I > 2\sigma(I)$.

Symmetry-equivalent data for **1** and **2** were averaged with R = 0.0414 and 0.0361, respectively, to give 2614 and 2842 independent reflections from a total 5068 and 3023 collected. The structures were solved by direct methods using SHELXS-86[5a] and refined by full-matrix least-squares techniques on F^2 with SHELXL-93[5b] using 2609 (**1**) and 2838 (**2**) reflections and refining 259 and 273 parameters, respectively. Hydrogen atoms for **1** were located by difference maps (except those of the disordered methyl group of the coordinated methoxide, which were introduced at calculated positions as riding on their bonded atom) and refined isotropically. All non-hydrogen atoms were refined anisotropically. All hydrogen atoms of **2** were located by difference maps and refined isotropically. All non-hydrogen atoms (except the oxygen atoms of the perchlorate ion, which were found disordered and refined isotropically in two different orientations) were refined anisotropically. The final values of *R*1 and w*R*2 for observed data are listed in Table 1. The maximum and minimum residual peaks in the final difference map were 0.653 and −0.410 e Å^{-3} for **1** and 0.714 and −0.746 e Å^{-3} for **2**. The largest shifts/esd in the final cycle were 1.414 for **1** and 0.112 for **2**.

Results and Discussion

Syntheses and Spectroscopic Characterization. The present work represents one of the first stages of a program concerned with developing synthetic methodologies to high-nuclearity M_x (M = Mn, Fe, Co, Ni, Cu; $x \geq 4$) clusters with interesting structural, spectroscopic, and magnetic properties, and it takes advantage of the observation that the reactions between metal carboxylates and dpk are proven to be a rich source of such products. Thus, for example, the $[Cu_2(O_2CCH_3)_4(H_2O)_2]$/dpk/$ClO_4^-$ reaction mixture in H_2O yields[6] the remarkable octa-

(5) (a) Sheldrick, G. M. SHELXS-86: Structure Solving Program. University of Göttingen, Germany, 1986. (b) Sheldrick, G. M. SHELXL-93: Crystal Structure Refinement. University of Göttingen, Germany, 1993.

(6) (a) Tangoulis, V.; Paschalidou, S.; Bakalbassis, E. G.; Perlepes, S. P.; Raptopoulou, C. P.; Terzis, A. *Chem. Commun.* **1996**, 1297. (b) Tangoulis, V.; Raptopoulou, C. P.; Terzis, A.; Paschalidou, S.; Perlepes, S. P.; Bakalbassis, E. G. *Inorg. Chem.*, in press.

nuclear complex $[Cu_8(dpk{\cdot}OH)_8(O_2CCH_3)_4](ClO_4)_4{\cdot}9H_2O$ (**3**) ($dpk{\cdot}OH^-$ = the monoanion of the hydrated, gem diol form of di-2-pyridyl ketone), whereas the reactions between $[Cu_2(O_2CCH_3)_4(H_2O)_2]$ and dpk in MeCN, in the absence of counterions, give[7] the novel molecules $[Cu_7(OH)_2(dpk{\cdot}O)_3(O_2CCH_3)_6]$ (**4**) and $[Cu_{12}(dpk{\cdot}O)_6(O_2CCH_3)_{12}]$ (**5**), where $dpk{\cdot}O^{2-}$ is the doubly deprotonated anion of the gem diol form of di-2-pyridyl ketone. Our recent success with the synthesis and characterization of the above polynuclear species prompted us to extend this work to analogous reaction mixtures in alcohols.

The preparation of compound **1** can be achieved via the 1:2:1 reaction of $[Cu_2(O_2CCH_3)_4(H_2O)_2]$ with dpk and $NaClO_4$ in MeOH. This preparation can be summarized by eq 1. The same

$$2[Cu_2(O_2CCH_3)_4(H_2O)_2] + 4dpk + 6CH_3OH + 2NaClO_4 \xrightarrow{CH_3OH} \underset{\mathbf{1}}{[Cu_4(dpk{\cdot}CH_3O)_4(CH_3O)_2](ClO_4)_2} + 2NaO_2CCH_3 + 6CH_3CO_2H + 4H_2O \quad (1)$$

product can be isolated from the 1:2:2 and 1:4:4 stoichiometries. It is well-known[8] that the carbonyl group of dpk, when coordinated to metal ions usually adds a protic molecule, HX (X = OH, CH_3O, ...), to give dpk·HX, while in general such addition products of ketones are rather unstable and exist only when the carbonyl group is flanked by strong electron-withdrawing groups. Several reasons for this behavior have been presented.[8m,l,9] The neutral dpk·HX and anionic $dpk{\cdot}X^-$ ligands, as well as the $dpk{\cdot}O^{2-}$ dianion, have been shown by X-ray analyses to be capable of binding to transition metals in a number of different ways.[6−8]

In a subsequent experiment, it was discovered that the, at first glance, trivial replacement of MeOH with EtOH led to the completely different product $[Cu_3(dpk{\cdot}C_2H_5O)_3(C_2H_5OH)_3](ClO_4)_3$ (**6**); the synthesis, X-ray structure, and full magnetic characterization of this trinuclear complex will be reported in due course.

The violet mononuclear complex **2** can be obtained readily by the reaction of $Cu(ClO_4)_2{\cdot}6H_2O$ with dpk in a 1:2 ratio in MeOH.

Complex **1** hydrolyzes in moist air to give a blue powder, the elemental composition and IR spectroscopic properties of which are consistent with the empirical formulation $Cu_4(dpk{\cdot}CH_3O)_4(OH)_2(H_2O)_2(ClO_4)_2$. The substitution of methoxide by hydroxide in the solid state has been observed.[10] Attempts to obtain this solid in a form suitable for crystallography failed. Compound **1** appears to be slightly soluble in hot MeOH and decomposes in DMF, yielding a green solution. Complex **2** is soluble in organic solvents, but to varying extents.

In the IR spectra, a dried sample of complex **2** exhibits a broad medium-intensity band at 3456 cm^{-1}, assignable to $\nu(OH)_{dpk{\cdot}CH_3O^-}$.[11] The spectra of both complexes do not exhibit a band in the region expected for $\nu(C{=}O)$ absorption (1684 cm^{-1} for free dpk), with the nearest band at 1605 cm^{-1}, assigned as a pyridine stretching mode raised from 1582 cm^{-1} on coordination, as observed earlier[8l] on complex formation involving hydration of dpk. The strong band of **1** at 1052 cm^{-1} is assigned to the C−O stretching vibration of the bridging methoxy group.[12] The spectra exhibit a very strong band at ∼1100 and a medium band at ∼625 cm^{-1} due to the $\nu_3(F_2)$ and $\nu_4(F_2)$ modes of the uncoordinated ClO_4^-, respectively.[11] Examination of the far-IR spectrum of **1** in the 400−200 cm^{-1} region reveals five metal-dependent stretching vibrations. The vibrations at 396 and 338 cm^{-1} can be assigned to Cu−N stretching modes, while the absorptions at 277, 261, and 230 cm^{-1} are assigned to Cu−O stretching vibrations.[13]

The d−d spectrum of **2** in MeOH consists of a featureless band at 596 nm; this wavelength is typical of a distorted *trans*-$Cu^{II}N_4O_2$ chromophore.[14] The complex also exhibits an absorption at 335 nm assignable to an $O_{dpk{\cdot}CH_3OH}$-to-Cu^{II} LMCT transition.[14]

Description of Structures. ORTEP plots of the cations of **1** and **2** are shown in Figures 1 and 2, respectively. Selected bond distances and angles are listed in Tables 2 and 3.

The four Cu^{II} atoms in the cationic unit of **1** are coplanar, showing the rare rhombic arrangement. The most common arrangement of tetranuclear Cu(II) compounds is tetrahedral.[15] To our knowledge, there are a few more examples of an approximate rectangular planar arrangement of tetranuclear Cu(II) compounds with the metal atoms in close proximity.[1,16] The central Cu_4O_4 core of the cation of **1** is composed of two crystallographically independent Cu^{II} atoms (namely Cu(1) and Cu(2)) lying on perpendicular 2-fold symmetry axes and one alkoxo-type oxygen atom of the $dpk{\cdot}CH_3O^-$ ligand. All eight atoms of the Cu_4O_4 core are coplanar within experimental error.

(7) Tangoulis, V.; Paschalidou, S.; Bakalbassis, E. G.; Perlepes, S. P.; Raptopoulou, C. P.; Terzis, A. *Angew. Chem., Int. Ed. Engl.* **1997**, *36*, 1083.

(8) (a) Jensen, W. P.; Hamza, A. I.; Suh, I.-H.; Jacobson, R. A.; Sommerer, S. O. *Inorg. Chim. Acta* **1997**, *254*, 367. (b) Deveson, A. C.; Heath, S. L.; Harding, C. J.; Powell, A. K. *J. Chem. Soc., Dalton Trans.* **1996**, 3173. (c) Kavounis, C. A.; Tsiamis, C.; Cardin, C. J.; Zubavichus, Y. *Polyhedron* **1996**, *15*, 385. (d) Alonzo, G.; Bertazzi, N.; Maggio, F.; Benetollo, F.; Bombieri, G. *Polyhedron* **1996**, *15*, 4269. (e) Papadopoulos, A.; Tangoulis, V.; Raptopoulou, C. P.; Terzis, A.; Kessissoglou, D. P. *Inorg. Chem.* **1996**, *35*, 559. (f) Breeze, S. R.; Wang, S.; Greedan, J. E.; Raju, N. P. *Inorg. Chem.* **1996**, *35*, 6944. (g) Sommerer, S. O.; Abboud, K. A. *Acta Crystallogr., Sect. C* **1993**, *49*, 1152. (h) Sommerer, S. O.; Baker, J. D.; Jensen, W. P.; Hamza, A.; Jacobson, R. A. *Inorg. Chim. Acta* **1993**, *210*, 173. (i) Baggio, R.; Gonzàlez, O.; Garland, M. T.; Manzur, J.; Acuna, V.; Atria, A. M.; Spodine, E.; Pena, O. *J. Crystallogr. Spectrosc. Res.* **1993**, *23*, 749. (j) Sommerer, S.; Jensen, W. P.; Jacobson, R. A. *Inorg. Chim. Acta* **1990**, *172*, 3. (k) Wang, S.-L.; Richardson, J. W., Jr.; Briggs, S. J.; Jacobson, R. A.; Jensen, W. P. *Inorg. Chim. Acta* **1986**, *111*, 67. (l) Byers, P. K.; Canty, A. J.; Engelhardt, L. M.; Patrick, J. M.; White, A. H. *J. Chem. Soc., Dalton Trans.* **1985**, 981. (m) Annibale, G.; Canovese, L.; Cattalini, L.; Natile, G.; Biagini-Cingi, M.; Manotti-Lanfredi, A.-M.; Tiripicchio, A. *J. Chem. Soc., Dalton Trans.* **1981**, 2280.

(9) (a) Fischer, B. E.; Sigel, H. *J. Inorg. Nucl. Chem.* **1975**, *37*, 2127. (b) Feller, M. C.; Robson, R. *Aust. J. Chem.* **1970**, *23*, 1997. (c) Feller, M. C.; Robson, R. *Aust. J. Chem.* **1968**, *21*, 2919.

(10) Taft, K. L.; Delfs, C. D.; Papaefthymiou, G. C.; Foner, S.; Gatteschi, D.; Lippard, S. J. *J. Am. Chem. Soc.* **1994**, *116*, 823.

(11) Nakamoto, K. *Infrared and Raman Spectra of Inorganic and Coordination Compounds*, 4th ed.; Wiley: New York, 1986; pp 231, 251, 253.

(12) Hall, L. A. P. M. *Polyhedron* **1990**, *9*, 2575.

(13) (a) van Albada, G. A.; Lakin, M. T.; Veldman, N.; Spek, A. L.; Reedijk, J. *Inorg. Chem.* **1995**, *34*, 4910. (b) Ghomashchi, E. *Spectrosc. Lett.* **1994**, *27*, 829.

(14) Lever, A. B. P. *Inorganic Electronic Spectroscopy*, 2nd ed.; Elsevier: Amsterdam, 1984; pp 311, 356, 554−572.

(15) (a) Hathaway, B. J. In *Comprehensive Coordination Chemistry*; Wilkinson, G., Gillard, R. D., McCleverty, J. A., Eds.; Pergamon Press : Oxford, England, 1987; Vol. 5, Chapter 53. (b) Melnik, *M. Coord. Chem. Rev.* **1982**, *42*, 259.

(16) (a) Castro, I.; Sletten, J.; Calatayud, M. L.; Julve, M.; Cano, J.; Lloret, F.; Caneschi, A. *Inorg. Chem.* **1995**, *34*, 4903. (b) Samules, J. A.; Chiang, W.-C.; Huffman, J. C.; Trojan, K. L.; Hatfield, W. E.; Baxter, D. V.; Caulton, K. G. *Inorg. Chem.* **1994**, *33*, 2167. (c) Reim, J.; Krebs, B. *Angew. Chem., Int. Ed. Engl.* **1994**, *33*, 1969. (d) Chaudhuri, P.; Karpenstein, I.; Winter, M.; Lengen, M.; Butzlaff, C.; Bill, E.; Trautwein, A. X.; Flörke, U.; Haupt, H.-J. *Inorg. Chem.* **1993**, *32*, 888. (e) Tandon, S. S.; Mandal, S. K.; Thompson, L. K.; Hynes, R. C. *Inorg. Chem.* **1992**, *31*, 2215. (f) McKee, V.; Tandon, S. S. *J. Chem. Soc., Dalton Trans.* **1991**, 221. (g) Kolks, G.; Lippard, S. J.; Waszczak, J. V.; Lilienthal, H. R. *J. Am. Chem. Soc.* **1982**, *104*, 717. (h) ten Hoedt, R. W. M.; Hulsberen, F. B.; Verschoor, G. C.; Reedijk, J. *Inorg. Chem.* **1982**, *21*, 2369. (i) Little, R. G.; Moreland, J. A.; Yawney, D. B. W.; Doedens, R. J. *J. Am. Chem. Soc.* **1974**, *96*, 3384.

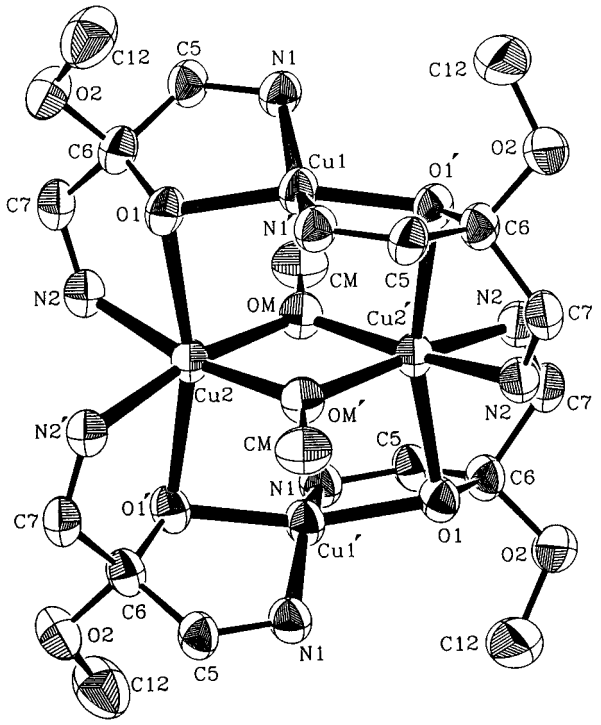

Figure 1. ORTEP diagram of the cation of **1** with 50% thermal probability ellipsoids showing the atomic labeling scheme. For clarity, we have primed only the atoms used in the discussion (see text) and most carbon atoms of the pyridyl rings have been omitted.

Table 2. Selected Interatomic Distances (Å) and Angles (deg) for Complex **1**[a,b]

		Distances	
Cu(1)−O(1)	1.891(4)	Cu(1)···Cu(2)	3.108(1)
Cu(1)−N(1)	1.968(5)	Cu(1)···Cu(1′)	5.377(1)[a]
Cu(2)−O(1)	2.412(4)	Cu(2)···Cu(2′)	3.120(1)[b]
Cu(2)−N(2)	2.029(4)		
Cu(2)−O(M)	1.961(3)		
		Angles	
O(1)−Cu(1)−O(1′)	162.0(2)[a]	O(1)−Cu(2)−N(2)	95.0(2)
O(1)−Cu(1)−N(1)	84.3(2)	O(1)−Cu(2)−O(M)	96.5(1)
O(1′)−Cu(1)−N(1)	100.1(2)[a]	O(1)−Cu(2)−O(1′)	165.4(2)[b]
N(1)−Cu(1)−N(1′)	152.1(3)[a]	N(2)−Cu(2)−O(M)	99.2(2)
		N(2)−Cu(2)−O(M′)	168.6(1)[a]
Cu(1)−O(1)−Cu(2)	91.7(1)	N(2)−Cu(2)−N(2′)	88.5(3)[b]
Cu(2)−O(M′)−Cu(2′)	105.4(2)[b]	O(M)−Cu(2)−O(M′)	74.6(2)[a]
		O(M)−Cu(2)−O(1′)	95.1(1)[b]
		O(1)−Cu(2)−N(2′)	74.4(2)[b]

[a] Symmetry transformation: $1 - x$, $0.5 - y$, z. [b] Symmetry transformation: $0.25 + y$, $x - 0.25$, $0.75 - z$.

Perpendicular to the plane of the Cu_4O_4 central core is the mean plane of the $Cu_2(OM)_2$ core, where O(M) is the oxygen atom of the CH_3O^- ligand. The interatomic distances between the crystallographically independent Cu^{II} atoms (Cu(1)···Cu(2)), which constitute the sides of the rhombus, are all equal to 3.108(1) Å. The two diagonals of the rhombus correspond to the interatomic distances Cu(1)···Cu(1′) and Cu(2)···Cu(2′) and are equal to 5.377(1) and 3.120(1) Å, respectively, the short diagonal being almost identical to the sides of the rhombus. Consequently, the four Cu^{II} atoms in the cluster could be considered as originating from two equilateral triangles sharing a common edge. The complex $[Cu_4(tfa)_2(ttpt)_2(5\text{-Hmpz})_4]$ (Htfa = trifluoroacetic acid; H_3ttpt = 2,4,6-tris(trifluoromethyl)-tetrahydropyran-2,4,6-triol; 5-Hmpz = 5-methyl-1*H*-pyrazole)[17a] comes closest to reproducing the topological arrangement of the Cu^{II} atoms in **1**. In the former complex, however, there are two pairs of equal sides in the rhombus (3.146(2), 3.181(2) Å),

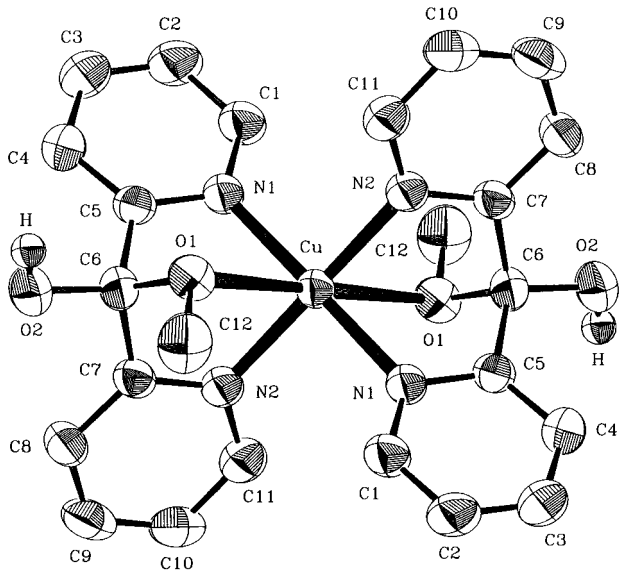

Figure 2. ORTEP diagram of the cation of **2** with 50% thermal probability ellipsoids showing the atomic labeling scheme.

the two diagonals being 2.943(2) and 5.601(3) Å. Another tetranuclear complex is somewhat structurally related to compound **1** in that it also exhibits a rhombic arrangement of the metal ions: $[Cu_2^{II}Cu_2^{I}(maamt)Cl_6]$ (maamt = 4-amino-3,5-bis-[(methylamino)methyl]-1,2,4-triazole); in this mixed-valence cluster[17b] the sides of the rhombus are 3.875(1) and 4.022(1) Å, the two diagonals being 4.084(1) and 6.782(1) Å.

The monoanion of the dpk·CH_3O^- ligand is coordinated to two different Cu^{II} atoms (Cu(1) and Cu(2)) through the pyridyl nitrogen atoms (N(1) and N(2)) while the deprotonated alkoxo oxygen atom (O(1)) is the bridging atom between Cu(1) and Cu(2). The methylated oxygen atom of dpk·CH_3O^- ligand remains unbound to the metals. The dpk·CH_3O^- ligand acts as a $\eta^1{:}\eta^2{:}\eta^1{:}\mu_2$ ligand, forming two CuNCCO five-membered chelating rings with two different metals. This ligation mode has also been observed in the crystal structures of $[Zn_2(dpk\cdot CH_3O)_2(NO_3)_2]$,[8b] $[Cu_2(dpk\cdot CH_3O)Cl_3]_n$,[8b] and $[Cu_4(dpk\cdot CH_3O)_2Cl_6]_n$.[8e] The symmetrically equivalent Cu(2) atoms are bridged through the oxygen atom (O(M)) of the deprotonated coordinated methanol molecule. No bridging exists between the symmetrically relevant Cu(1) atoms. The two CuNCCO rings are planar within experimental error, forming an angle of 71°. The pyridyl rings of the same dpk·CH_3O^- ligand present a dihedral angle of 70.6° as compared to 180° for a planar ligand.

The coordination sphere around Cu(1) can be described as distorted square planar consisting of two nitrogen (N(1)) and two alkoxo oxygen (O(1)) atoms of two different dpk·CH_3O^- ligands. The Cu(2) atom presents an axially elongated distorted octahedral coordination geometry consisting of two nitrogen (N(2)) atoms of two different dpk·CH_3O^- ligands and two methoxo oxygen (O(M)) atoms in the equatorial plane, while the axial positions are occupied by alkoxo oxygen (O(1)) atoms of two different dpk·CH_3O^- ligands. The average Cu−N bond distance is 1.999 Å (Cu(1)−N(1) = 1.968(5) Å, Cu(2)−N(2) = 2.029(4) Å), while the average equatorial Cu−O bond length is 1.926 Å (Cu(1)−O(1) = 1.891(4) Å, Cu(2)−O(M) = 1.961(3) Å), about 0.5 Å shorter than the corresponding axial bond distance (Cu(2)−O(1) = 2.412(4) Å).

The asymmetric unit of complex **2** contains half of the mononuclear $[Cu(dpk\cdot CH_3OH)_2]^{2+}$ cation, one ClO_4^- counter-

(17) (a) Kogane, T.; Harada, K.; Hirota, R.; Urushiyama, A. *Polyhedron* **1996**, *15*, 4093. (b) van Koningsbruggen, P. J.; Haasnoot, J. G.; Kooijman, H.; Reedijk, J.; Spek, A. L. *Inorg. Chem.* **1997**, *36*, 2487.

Table 3. Selected Interatomic Distances (Å) and Angles (deg) for Complex **2**

	Distances		
Cu−N(1)	2.007(4)	C(6)−O(1)	1.436(6)
Cu−N(2)	1.999(4)	C(6)−O(2)	1.380(6)
Cu−O(1)	2.470(3)		
	Angles		
N(1)−Cu−N(2)	87.8(2)	N(2)−Cu−O(1)	75.6(1)
N(1)−Cu−O(1)	107.8(1)	C(6)−O(1)−C(12)	113.8(4)

Hydrogen Bonds[a−c]

D	H	A	D···A, Å	D−H···A, deg
O(2)	H(O(2))	O(7)[i]	2.66	159.5
O(7)	H(O(7))	O(5)[ii]	2.84	154.3

[a] Symmetry operations: (i) $0.5 - x$, $0.5 - y$, $z - 1$; (ii) $0.5 + x$, $0.5 - y$, $1 + z$. [b] A = acceptor, D = donor. [c] Atoms O(5) and O(7) belong to the perchlorate counterion and solvate methanol, respectively.

ion, and one methanol solvate molecule; the last two will not be further discussed. The most interesting feature of the structure is the coordination of the methylated oxygen of the dpk·CH_3OH ligand, while the hydroxyl oxygen atom remains protonated and unbound to the metal.

Compound **2** has an inversion center. The neutral ligand is coordinated to the copper center as a tridentate chelate via two nitrogen and one oxygen atoms. The geometry of the copper(II) ion is elongated octahedral. The pyridyl nitrogens can be viewed as strongly coordinating to the metal (Cu−N = 1.999(4) and 2.007(4) Å), while the methylated oxygen forms a weak bond to Cu^{II} (Cu−O(1) = 2.470(3) Å) in the axial direction. This ligation mode of dpk·CH_3OH was observed in the recently reported[8b,c] structure of [$CuCl_2$(dpk·CH_3OH)].

The two pyridyl rings of the dpk·CH_3OH ligand are planar and form a dihedral angle of 66.9° (N(1)C(1)C(2)C(3)C(4)C(5)/N(2)C(7)C(8)C(9)C(10)C(11)). The two five-membered chelating rings, Cu−N(1)−C(5)−C(6)−O(1) and Cu−N(2)−C(7)−C(6)−O(1), exist in the envelope form where the O(1) atom is 1.07 and 1.04 Å out of the plane of the remaining four atoms, respectively. The dihedral angle formed between the mean planes CuN(1)C(5)C(6) and CuN(2)C(7)C(6) is 62.9°. The six-membered ring, Cu−N(1)−C(5)−C(6)−C(7)−N(2), is in the boat conformation, with the Cu and C(6) atoms being 0.98 and 0.73 Å, respectively, out of the best mean plane passing through N(1), C(5), C(7), and N(2). There is also a hydrogen-bonding network among the CH_3OH molecule, the ClO_4^- counterion, and the hydroxyl group of dpk·CH_3OH (Table 3).

The structure of the cation of **2**, as detailed in the discussion above and in Table 3, shows remarkable similarity to those[8k] of the cations of [Cu(dpk·H_2O)$_2$]Cl_2·$4H_2O$ and [Cu(dpk·H_2O)$_2$]-(NO_3)$_2$·$2H_2O$.

Magnetic and EPR Properties of Complex 1. Variable-temperature (3−300 K) magnetic susceptibility data were collected for a solid sample of **1**. The temperature dependence of the $\chi_M T$ product of **1**−χ_M being the corrected molar magnetic susceptibility per tetramer and T the absolute temperature—shown in Figure 3, exhibits three different features in the high (300−175 K), middle (175−50 K), and low (50−3 K) temperature range. In particular, the room temperature value of $\chi_M T$ (0.835 cm^3 K mol^{-1}) is much smaller than that expected for four uncoupled $S = {}^1/_2$ spins (1.5 cm^3 K mol^{-1}), indicative of strong antiferromagnetic coupling; it decreases rapidly with decreasing temperature down to 175 K. Below *ca.* 175 K, the value is stabilized at about 0.795 cm^3 K mol^{-1}, corresponding to two uncoupled doublets, and below *ca.* 50 K, it starts to decrease again, reaching the value of 0.735 cm^3 K mol^{-1} at 3 K.

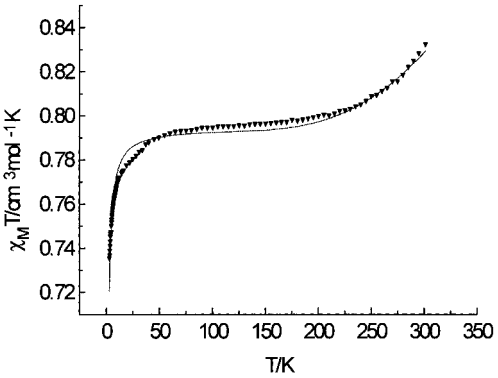

Figure 3. Plot of $\chi_M T$ /Cu_4^{II} vs T for a polycrystalline sample of complex **1**: (▲), experimental data; solid line, best fit of eq 4.

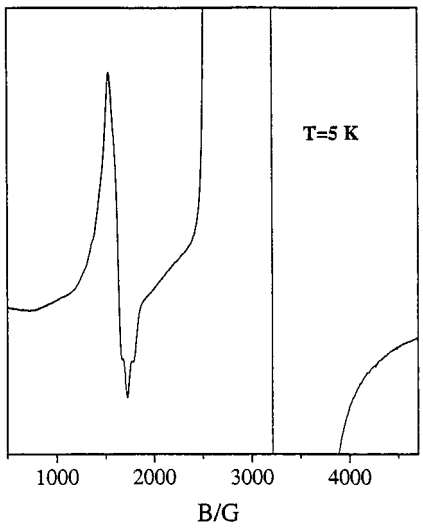

Figure 4. X-band EPR spectrum of a polycrystalline sample of **1** at 5 K.

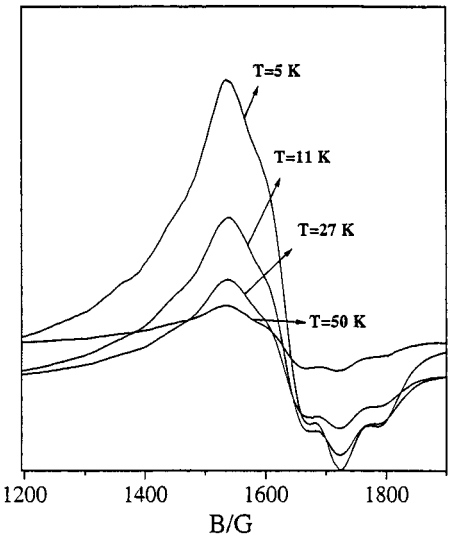

Figure 5. Temperature dependence (5 −50 K) of the half-field transition of the X-band powder EPR spectrum of **1**.

Powder EPR spectra of **1** were recorded at a wide range of temperatures (295−5 K). At 5 K (Figure 4), **1** shows two features centered at 1600 and 3200 G, respectively. Moreover, the intensity of the former decreases on increasing temperature (Figure 5), whereas new features at 1000 and 4000 G appear at room temperature (Figure 6).

The first decrease of $\chi_M T$ with decreasing temperature, along with the plateau close to 0.8 cm^3 K mol^{-1} and the final decrease

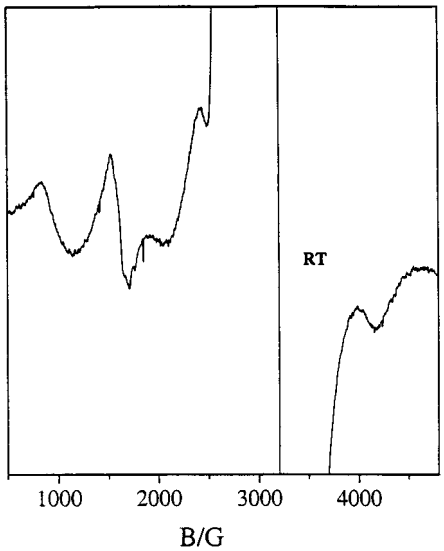

Figure 6. X-band EPR spectrum of a polycrystalline sample of **1** at room temperature.

Scheme 1. The Exchange Pathways in **1**[a]

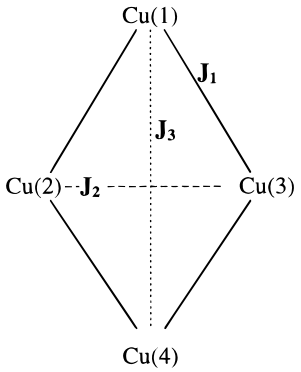

[a] Atoms Cu(3) and Cu(4) of this diagram correspond to atoms Cu(2′) and Cu(1′), respectively, of the real structure shown in Figure 1.

below 50 K, is a clear indication that several exchange pathways of different efficiency operate in the tetramer.[18] A possible explanation for this could be that at least one exchange pathway is so strong that the two spins connected by it are in a singlet ground state at 175 K. Therefore, the final decrease could be interpreted as the effect of other exchange pathways which become important below 50 K. This latter hypothesis is confirmed by the temperature dependence of the EPR spectra. Hence, it must be assumed that at least one of the three parameters, J_1, J_2, and J_3 shown in Scheme 1, in which a new numbering for the Cu(2′) and Cu(1′) magnetic centers of Figure 1 is used, is very effective in transmitting strong antiferromagnetic coupling. However, an inspection of the molecular structure of **1** clearly shows that the main exchange parameter should be J_2, because this pathway is through the bis(μ-alkoxo) bridge between Cu(2) and Cu(3) and has (a) a short Cu(2)···Cu(3) distance (3.12 Å) and (b) two large Cu−O−Cu angles of 105.4(2)°. J_1 cannot be expected to be the main exchange parameter because the peripheral pathway, while displaying the same metal−metal distance, Cu(1)···Cu(3) = 3.11 Å, has a small Cu−O−Cu angle of 91.7(1)° and is through a single μ-alkoxo bridge. Since it is well-known that a bis(μ-alkoxo) bridge is more effective than a single one in transmitting strong antiferromagnetic coupling,[18] we will accept J_2 as the main exchange parameter. Finally, the Cu(1)···Cu(4) diagonal interaction is expected to be very weak due to the very long Cu···Cu distance (5.38 Å).

Assuming that J_2 is much larger than the other coupling constants, we will try next to interpret the magnetic properties of **1**. Whether or not this is a reasonable assumption must be verified a posteriori by the ability of the model to reproduce the experimental $\chi_M T$ versus T plot.

If J_2 is much larger than all the other coupling constants, then the high-temperature part of the magnetic susceptibility data will only be due to the splitting of the spin levels introduced by this stronger interaction. In this case, the lowest energy level is the one with the pair Cu(2) and Cu(3) (Scheme 1) in its ground $S = 0$ state and the Cu(1) and Cu(4) ions independent. Consequently, a first model to explain the magnetic behavior of **1** in the 300−50 K temperature range could be that in which the molar susceptibility of the system, χ_M(4Cu), is given as a sum of two isolated doublets, χ_{Cu}, and two coupled Cu(II) ions (Bleaney−Bowers model[19]), χ_{BB}, i.e.

$$\chi_M(4Cu) = 2\chi_{Cu} + \chi_{BB} \quad (2)$$

A very good fit ($R = \sum_n[(\chi_M T)_{exp} - (\chi_M T)_{calc}]^2 = 1.8 \times 10^{-4}$; TIP was fixed at 60×10^{-6} cm^3 mol^{-1}) was derived with $2J = -950(10)$ cm^{-1}, $C = 0.39$ K, and $g = 2.10(1)$ (see Supporting Information, Figure 1S), in agreement with the experimental indications for the existence of a strong antiferromagnetic coupling between two copper(II) ions.

However, the low-temperature behavior of the susceptibility could be described by considering also weaker interactions. As a consequence, in an attempt to interpret the experimental magnetic susceptibility data of **1** as a whole, the zero-field Hamiltonian should be as follows:[3]

$$H = -2J_1(S_1 \cdot S_2 + S_3 \cdot S_4 + S_4 \cdot S_2 + S_3 \cdot S_1) - 2J_2(S_2 \cdot S_3) - 2J_3(S_1 \cdot S_4) \quad (3)$$

This Hamiltonian is diagonal in a basis consisting of eigenvectors of S^2, S_{23}^2, and S_{14}^2 where S is the total spin, $S_{23} = S_2 + S_3$, and $S_{14} = S_1 + S_4$. The energy levels (with a suitable choice of the zero level) are given by the expression

$$E(S,S_{23},S_{14}) = -J_1 S(S+1) - (J_2 - J_1)S_{23}(S_{23}+1) - (J_3 - J_1)S_{14}(S_{14}+1) \quad (4)$$

where $S = 0, 1, 2$, $S_{23} = 0, 1$, and $S_{14} = 0, 1$, such that $|S_{23} - S_{14}| \le S \le S_{23} + S_{14}$.

Hence, the 3−300 K experimental data were fitted next, by using the following resulting theoretical expression for the magnetic susceptibility:

$$\chi_M = \frac{Ng^2\mu_B^2}{3kT} \frac{\sum_i (2S_i+1)S_i(S_i+1)\exp(-E_i/kT)}{\sum_i (2S_i+1)\exp(-E_i/kT)} \quad (5)$$

The obtained values are $J_1 = +22(4)$ cm^{-1}, $J_2 = -490(9)$ cm^{-1}, $g = 2.058(2)$, $J_3 = -0.36(1)$ cm^{-1}, and $R = 1.5 \times 10^{-3}$. This fit is shown in Figure 3 (solid line). It should be stressed here that the J_2 value is very close to the corresponding one ($J = -475$ cm^{-1}) derived from the previous model and the theoretical g value is almost identical to the experimental one ($g_{iso} = 2.054$) of the mononuclear complex **2**, supporting the correctness of the models used.

The energy spectrum with this set of parameters is shown in Scheme 2. Scheme 2 reveals that the ground state is a singlet

(18) Barra, A.-L.; Gatteschi, D.; Pardi, L.; Müller, A.; Döring, J. *J. Am. Chem. Soc.* **1992**, *114*, 8509.

(19) Bleaney, B.; Bowers, K. D. *Proc. R. Soc. London, Ser. A* **1952**, *214*, 451.

Scheme 2. Energy Levels of **1**, Based on Eq 4

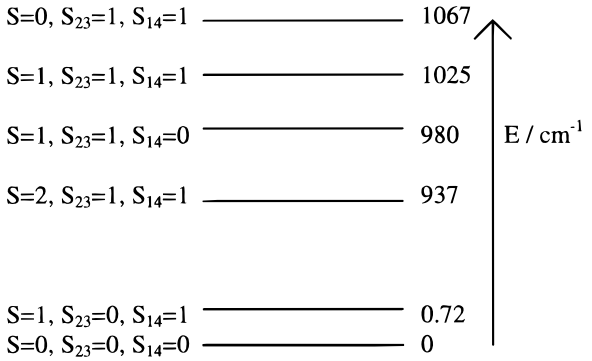

whereas a triplet one is very close in energy, their energy gap being only 0.72 cm^{-1}. The next excited level, $S = 2$, is 937 cm^{-1} higher from the ground state, showing that, even at room temperature, essentially only the two lowest levels are populated.

The magnetization of **1** *vs* BT^{-1} at 3 K and in the 0−5 T field range is shown in Figure 7. Figure 7 shows that the experimental magnetization curve (dotted line) reaches a value of 1.58 μ_B at 5 T. The other two lines represent the theoretical magnetization behavior of an $S = 1$ system (dashed line) and a system of two isolated doublets (solid line). Both have been calculated from the expression

$$M = Ng\mu_B SB_S(x) \qquad (6)$$

where $B_S(x)$ is the Brillouin function for states with $S = 1$ and $S = 2 \times {}^1/_2$, respectively. Figure 7 clearly shows that (i) at 3 K a singlet and a triplet state are populated (as it was also shown from the susceptibility data) and (ii) the behavior of **1** can be simulated by two noncorrelated doublets, $S = {}^1/_2$, while the other pair of $S = {}^1/_2$ doublets are coupled strongly antiferromagnetically.

It is worth mentioning at this point that a 14.5−300 K data fit, by using a 2-*J* model, failed to yield a positive J_1 value and a good low-temperature fit.

The EPR spectrum at 5 K (Figure 4) shows a feature at 1600 G along with a main one, centered at 3200 G. The latter could be attributed to monomeric impurities, and the former, to a half-field transition. Moreover, the magnitude of the *D* splitting is estimated[20] to be ≤ 0.01 cm^{-1}. The intensity of the half-field transition—which appeared also at room temperature (Figure 6)—decreases while the temperature increases (Figure 5). All these observations are in line with our previous considerations concerning the population of the two lowest states. The two new features at 1000 and 4000 G, appearing at room temperature, are probably due to the population of other excited states.

Magnetostructural Correlation and Ground State Degeneration. The most common geometries of tetranuclear copper(II) complexes with planar arrangements are those of a rectangle and of a square. The main aspect of a rectangle is that the diagonal exchange pathways are almost negligible due to the long distance between the copper ions. However, the ground state of the planar tetranuclear copper(II) complexes with nonzero diagonal interactions is a singlet, without orbital degeneration, while the first excited state is either a triplet or a degenerate triplet;[1,16a,b,e] still the energy difference between the ground and the first excited state is much larger than in our case. In an attempt to probe deeper into the magnetic exchange interactions of **1**, its magnetic behavior is closely combined with its molecular and crystal structure. As was shown in a previous section, **1** has a very interesting structure, built from planar tetranuclear copper(II) molecules, in which the four magnetic ions occupy the apices of a rhombus. A more careful examination of the rhombus, however, clearly shows that its Cu^{II} atoms exhibit, in pairs, identical coordination spheres (Figure 1). In particular, the coordination sphere around each Cu(1)—due to the long Cu(1)-O(M) separation (2.940 Å)—could be better described as distorted square planar [CuN_2O_2], while that around each Cu(2) could be described as distorted octahedral [CuN_2O_4]. Consequently, the unpaired electron around each Cu(1) magnetic center is described by a $(x^2 - y^2)$-type magnetic orbital pointing from the metal toward its four nearest-neighboring N(1), N(1′), O(1), and O(1′) atoms. The unpaired electron around each Cu(2) magnetic center—due to both the long Cu(2)−O(1) separation (2.412 Å) and the C_{2v} site symmetry at Cu(2)—is described by a $(x^2 - y^2)$-type magnetic orbital pointing from the metal toward its four nearest-neighboring N(2), N(2′), O(M), and O(M′) atoms; hence, the spin density on O(1) and O(1′) atoms, originating from the Cu(2) ions, should be very low or zero. This latter point along with (i) the planar Cu(2)$(OM)_2$Cu(2′) moieties, (ii) the fact that both Cu(2)−O(M)−Cu(2′) angles (105.4°) are well above the transition angle (95.7°) established[21] experimentally for the alkoxo-bridged copper(II) complexes, and (iii) the Cu(2)···Cu(2′) bis(alkoxo) bridging character, could account well for the very strong Cu(2)···Cu(2′) interaction of $J_2 = -490(9)$ cm^{-1}, derived from the fitting procedure.

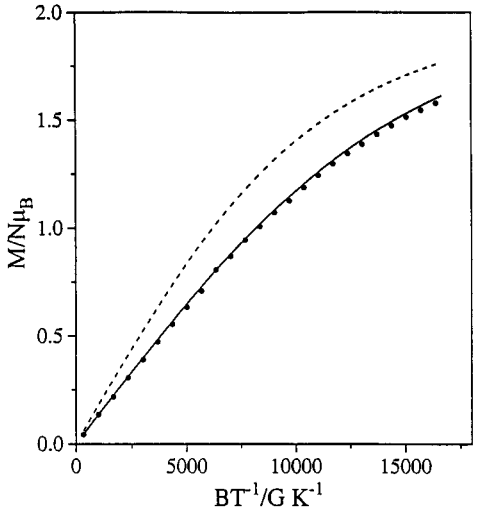

Figure 7. Isothermal (3 K) field dependence of magnetization of **1**. The dashed line represents the theoretical Brillouin function for an $S = 1$ system, and the solid line represents the theoretical Brillouin function for an uncoupled $S = {}^1/_2$, $S = {}^1/_2$ system.

The reliability of the peripheral J_1 value is examined next. The Cu(1)−O(1)−Cu(2) angle of 91.7° is well below the transition angle established experimentally for the alkoxo-bridged Cu$(OR)_2$Cu complexes, and each O(1) alkoxo bridging atom exhibits a triply bridging function. Moreover, contrary to the Cu(2)···Cu(2′) bis(alkoxo) bridging character, that between Cu(1) and Cu(2) is a single-alkoxo one. On this basis and because of the fact that antiferromagnetic interaction decreases as electron density is removed from bridging atoms,[22] a ferromagnetic interaction should be expected for the J_1 value, in fair agreement with the results of our fitting.

Finally, the almost degenerate ground state of **1** could be attributed to the very small energy difference—like that of *ca* 0.7 cm^{-1}, derived from the fitting procedure—and not to

(20) Bencini, A.; Gatteschi, D. *EPR of Exchange Coupled Systems*; Springer-Verlag: Heidelberg, Germany, 1990.

(21) Merz, L.; Haase, W. *J. Chem. Soc., Dalton Trans.* **1980**, 875.

(22) Hay, P. J.; Thibeault, J. C.; Hoffmann, R. *J. Am. Chem. Soc.* **1975**, *97*, 4884.

competing interactions (spin frustration[23]). The latter should be excluded because of the opposite signs derived for J_1 and J_2 from the fitting procedure. The reason for the almost degenerate $S = 0$ and $S = 1$ states is that the very strong J_2 interaction has paired the central spins of Cu(2) and Cu(3), leaving the two Cu(1) and Cu(4) ions almost noninteracting. In effect, at $T <$ 80 K, the exchange interaction between Cu(1) and Cu(4) can be interpereted by an undoubtedly very weak interaction, like the one ($J_3 = -0.4$ cm^{-1}) derived from the fitting procedure.

Conclusion. Our goal when beginning this work was to design high-nuclearity Cu(II) complexes. From this study and recent work in our group[6,7] (preparation and structural/magnetic characterization of a large variety of polynuclear metal assemblies with dpk·OH^-, dpk·O^{2-}, dpk·CH_3O^-, and dpk·$C_2H_5O^-$ as ligands), it is clear that the gem diol nature of the hydrated and alcoholated forms of di-2-pyridyl ketone makes them versatile ligands for use with a variety of metals and for a variety of objectives/advantages, including variable denticity levels, bridging vs terminal modes, high-nuclearity aggregate formation, and the linking of aggregates into polymeric arrays. Compound **1** described in this paper is actually a cluster with a nuclearity of 4. Moreover, the four copper(II) ions in the cluster could be considered as originating from two equilateral triangles sharing a common edge. Unlike the equilateral triangular Cu(II) complex,[4] the cluster under study does not exhibit spin frustration. Nevertheless, **1** constitutes a rare example of a magnetic system, allowing the determination of all its magnetic parameters, ranging from very strong to very weak.

Acknowledgment. This work was supported by the Greek General Secretariat of Research and Technology (PLATON Program 1583 to E.G.B. and Grant 91ED to S.P.P.), the Greek Secretariat of Athletics, OPAP (to A.T.), and Mrs. Athina Athanasiou (V.T.). We thank the reviewers for stimulating comments concerning the magnetochemistry of complex **1**. We are also indebted to Profs. O. Kahn (Laboratoire des Sciences Moleculaires, ICMCB, France) and G. Christou (Indiana University) for helpful discussions.

Supporting Information Available: Tables of magnetic susceptibility and magnetization data for **1** and a plot showing the best fit of $\chi_M T$ vs T data to eq 2 in the 300−50 K temperature range (Figure 1S) (4 pages). Two X-ray crystallographic files, in CIF format, are available on the Internet only. Ordering and access information is given on any current masthead page.

IC970332D

(23) (a) Kahn, O. *Molecular Magnetism*; VCH: New York, 1993. (b) Michaut, C.; Quahab, L.; Bergerat, P.; Kahn, O.; Bousseksou, A. *J. Am. Chem. Soc*. **1996**, *118*, 3160. (c) Kahn, O. *Phys. Lett*., in press.